# Flux-modulated tunable interaction regimes in two strongly nonlinear oscillators

J. D. Koenig,[1] G. Barbieri,[1] F. Fani Sani,[1] C. A. Potts,[1,2] M. Kounalakis,[1,3,*] and G. A. Steele[1]
[1]*Kavli Institute of Nanoscience, Delft University of Technology, PO Box 5046, 2600 GA Delft, The Netherlands*
[2]*Niels Bohr Institute, University of Copenhagen, Blegdamsvej 17, 2100 Copenhagen, Denmark*
[3]*Luxembourg Institute of Science and Technology (LIST), 4362 Esch-sur-Alzette, Luxembourg*

(Received 10 November 2025; accepted 19 January 2026; published 19 February 2026)

The ability to efficiently simulate a variety of interacting quantum systems on a single device is an overarching goal for digital and analog quantum simulators. In circuit quantum electrodynamical systems, strongly nonlinear superconducting oscillators are typically realized using transmon qubits, featuring a wide range of tunable couplings that are mainly achieved via flux-dependent inductive elements. Such controllability is highly desirable both for digital quantum information processing and for analog quantum simulations of various physical phenomena, such as arbitrary spin-spin interactions. Furthermore, broad tunability facilitates the study of driven-dissipative oscillator dynamics in previously unexplored parameter regimes. In this work, we demonstrate the ability to selectively activate different dynamical regimes between two strongly nonlinear oscillators using parametric modulation. In particular, our scheme enables access to regimes that are dominated by photon hopping, two-mode squeezing, or cross-Kerr interactions. Finally, we observe level repulsion and attraction between Kerr-nonlinear oscillators in regimes where the nonlinearities exceed the coupling strengths and decay rates of the system. Our results could be used for realizing purely analog quantum simulators to study arbitrary spin systems as well as for exploring strongly nonlinear oscillator dynamics in previously unexplored interaction regimes.

DOI: 10.1103/3pf2-8n9b

## I. INTRODUCTION

Quantum information processors based on superconducting circuits have long relied on the transmon qubit as a robust, reliable, and high-coherence building block in the journey toward large-scale digital quantum computation [1–3]. Circuit quantum electrodynamical (cQED) devices are also of great interest to the development of analog quantum simulators, in which devices are custom-built to emulate the behavior of distinct systems that are otherwise typically challenging to control or probe directly [4,5]. Such devices may enable the probing of physics in otherwise inaccessible parameter regimes due to the high degree of engineerability in superconducting circuits enabled by modern nanofabrication techniques and materials science [6,7].

Transmon-based cQED systems may be described as collections of coupled Kerr-nonlinear oscillators (KNOs), which in recent years have been imbued with *in situ* tunable resonance frequencies, couplings, and nonlinearities achievable by external control [8–11]. Tunable couplers have been successfully used to implement high-fidelity two-qubit gates, achieve exotic coupling regimes, and are useful elements for mitigating undesirable interactions in designs for scalable quantum computing architectures [12–22]. While such developments have contributed significantly to progress in digital gate-based architectures, there is still underexplored territory in using such platforms to emulate other interactions and physical systems such as extended Bose-Hubbard, arbitrary spin-spin, fractional Bloch oscillations, and lattice gauge theories [23–31]. Systems of coupled KNOs can be engineered to enable a variety of interactions, including intrinsic longitudinal and radiation-pressure-like couplings [32–34]. By introducing nonlinear coupling elements, many such interactions can be activated when driven or parametrically modulated [30,35,36]. Moreover, control over all $\sigma_X\sigma_X$, $\sigma_Y\sigma_Y$, and $\sigma_Z\sigma_Z$ couplings individually would allow for analog simulation of arbitrary XYZ spin-model Hamiltonians and coupled Ising spins [30,37,38]. Devices with couplers containing more highly nonlinear elements may also be used to enter into regimes where strictly nonlinear couplings such as correlated photon hopping and photon-pair tunneling terms dominate, allowing for the simulation of more exotic physics [39].

Here, we implement such flux-tunable interactions on a superconducting circuit containing two flux-tunable transmon qubits connected by a fixed capacitive coupling and a tunable nonlinear inductive coupling. The latter is realized using a superconducting quantum interference device (SQUID). By parametrically modulating the external flux threading the SQUID loop of the coupler, we operate the device in regimes where the longitudinal (cross-Kerr) coupling is dominant over a two-mode squeezing interaction and in which the single-photon exchange interaction (beam splitter) and

*Contact author: marios.kounalakis@gmail.com

*Published by the American Physical Society under the terms of the Creative Commons Attribution 4.0 International license. Further distribution of this work must maintain attribution to the author(s) and the published article's title, journal citation, and DOI.*

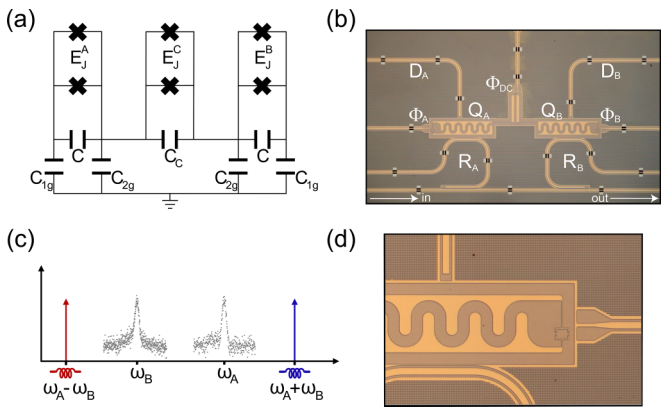


FIG. 1. Device and measurement scheme. (a) Circuit diagram for the device. On the left and right sides are two flux-tunable transmon qubits consisting of SQUIDs with gate capacitances to ground. The tunable coupler in the center consists of a coupling capacitor and a symmetric SQUID. (b) Optical microscope image of the device, including transmission line, readout resonators ($R_i$), drive lines ($D_i$), flux lines ($\Phi_i$), two transmons ($Q_i$), and the tunable coupler. (c) Schematic of the experiment. The flux incident on the coupler SQUID loop is modulated at either the difference or sum frequency of the two transmons. (d) Optical microscope image of qubit B.

cross-Kerr strengths are comparable. We observe two-mode squeezing effects through the use of parametric modulation, which, together with the single-photon hopping interaction, are characterized by level attraction and repulsion between the oscillators. While previous studies have explored such effects in linear systems [40–42], our system extends level attraction phenomena in KNOs. Our results pave the way for the realization of analog quantum simulators, based on nonlinear oscillators containing parametrically driven tunable couplers, to study exotic parameter regimes in nonlinear quantum systems.

## II. THEORETICAL ANALYSIS

The device comprised of two transmon qubits and a tunable coupler is shown in Fig. 1. The coupling between the two oscillators is solely characterized by the charging and Josephson energies of the constituent circuit elements. Both the linear and nonlinear interactions can be tuned via the total flux threading the coupler SQUID loop. The Josephson energy of the coupler is written as

$$E_J^C(\Phi_{\rm dc}) = E_{J\max}^C \left|\cos\left(\pi\frac{\Phi_{\rm dc}}{\Phi_0}\right)\right| \sqrt{1 + d_C^2 \tan^2\left(\pi\frac{\Phi_{\rm dc}}{\Phi_0}\right)}, \tag{1}$$

where $E_{J\max}^C$ is determined by the inductance of the unbiased SQUID loop, $d_C$ is a measure of the asymmetry of the junction inductances comprising the SQUID, and $\Phi_{\rm dc}$ is the dc flux threading the loop [1,43]. Each of the two transmons is capacitively coupled to its own coplanar waveguide readout resonator, which is in turn coupled to a common feedline through which the device is driven and probed. The Josephson energies of the two qubits are related to their own flux biases $\Phi_A$ and $\Phi_B$ in the same form as Eq. (1). In the coupled system, the ground to excited state transition frequency for transmon $i$ is given in units where $\hbar = 1$ as

$$\omega_i \approx \sqrt{8\widetilde{E}_J^i E_C^i} - E_C^i, \tag{2}$$

with $\widetilde{E}_J^i = E_J^i + E_J^C/4$ the modified Josephson energy due to the coupler and $E_C^i$ the charging energy of transmon $i$.

We obtain a full system Hamiltonian following the procedure outlined in the Supplemental Material [44] and Ref. [10]. We quantize the circuit shown in Fig. 1(a) and retain terms in the expansions of the energy potentials of the SQUIDs to fourth order. We can obtain a simplified Hamiltonian given by

$$\begin{aligned} H =& \omega_A \hat{a}^\dagger \hat{a} + \frac{\alpha_A}{2}\hat{a}^\dagger\hat{a}^\dagger\hat{a}\hat{a} + \omega_B \hat{b}^\dagger\hat{b} + \frac{\alpha_B}{2}\hat{b}^\dagger\hat{b}^\dagger\hat{b}\hat{b} \\ &+ J_1(\hat{a}^\dagger\hat{b} + \hat{a}\hat{b}^\dagger) + J_2(\hat{a}^\dagger\hat{b}^\dagger + \hat{a}\hat{b}) + V\hat{a}^\dagger\hat{a}\hat{b}^\dagger\hat{b}, \end{aligned} \tag{3}$$

where we have defined

$$J_{1,2} := \pm\left(\frac{\widetilde{E}_J^A\widetilde{E}_J^B E_C^A E_C^B}{4}\right)^{1/4} \left(\frac{E_C^C}{\sqrt{E_C^A E_C^B}} \mp \frac{E_J^C}{2\sqrt{\widetilde{E}_J^A\widetilde{E}_J^B}}\right) \tag{4}$$

and

$$V := -\frac{E_J^C}{8}\sqrt{\frac{E_C^A E_C^B}{\widetilde{E}_J^A\widetilde{E}_J^B}}, \tag{5}$$

where $J_1$ is the strength of the hopping interaction, $J_2$ is the squeezing, $V$ is the cross Kerr, $\alpha_i \approx -E_C^i$ the anharmonicity, and we have neglected higher-order terms which are far off-resonant from the relevant dynamics of the measurements performed. In systems of coupled Kerr-nonlinear oscillators, the two-mode squeezing term has been previously shown to produce nondegenerate parametric oscillations [45,46].

Under the rotating wave approximation (RWA) and when the two transmons are resonant, the single-photon hopping and cross-Kerr effects are observable with strengths $J_1$ and $V$, while the two-mode squeezing interaction is far off-resonant. In previous measurements on this device, the single-photon hopping and cross-Kerr interactions were shown to be highly tunable dependent on the choice of static coupler flux bias point with deep access to the regime $J_1 > V$ [10].

While the strengths of the linear and cross-Kerr couplings are ordinarily constrained by the engineered characteristics of the circuit and choice of flux bias point, by parametrically modulating the flux threading the SQUID loop of the coupler, one can access parameter regimes in which either the photon hopping or two-mode squeezing terms can be selectively activated. This selective activation enables one to induce—for even far off-resonant oscillators—linear interactions with strengths spanning a wide range of ratios $J_{1,2}/V$.

We consider the case in which the total magnetic flux threading the coupler contains a static dc component as well as a periodic ac component, where the total flux is given by

$$\Phi_C(t) = \Phi_{\rm dc} + \Phi_{\rm ac}\cos(\omega_m t) \tag{6}$$

and $\omega_m$ is the frequency of the modulation. Provided that the strength of modulation is small relative to the bias point [$\sin(\Phi_{\rm dc}) \gg \sin(\Phi_{\rm ac})$], we can insert Eq. (6) into Eq. (1) and obtain an expression for the Josephson energy of the coupler as

$$E_J^C(\Phi_C(t)) \approx E_{J\max}^C \left| \cos\left(\pi \frac{\Phi_{\rm dc}}{\Phi_0}\right) - \pi \frac{\Phi_{\rm ac}}{\Phi_0} \sin\left(\pi \frac{\Phi_{\rm dc}}{\Phi_0}\right) \times \cos(\omega_m t) \right| \sqrt{1 + d_c^2 \tan^2\left(\pi \frac{\Phi_{\rm dc}}{\Phi_0}\right)}$$
$$= E_{J,\rm dc}^C + E_{J,\rm ac}^C(t), \tag{7}$$

which is now comprised of a static term $E_{J,\rm dc}^C$ and a time-dependent term $E_{J,\rm ac}^C(t)$ due to the modulation.

After rederiving the expressions for the hopping and two-mode squeezing interactions, it can be found that by modulating the coupler at the difference or sum frequency $\omega_m = |\omega_A \pm \omega_B|$, either interaction can be selectively activated for nonresonant oscillators as the coupling strengths under modulation are modified to

$$J_1 \to [J_{1,\rm dc} + J_{\rm ac}(e^{i\omega_m t} + e^{-i\omega_m t})] \times (\hat{a}^\dagger \hat{b} e^{i(\omega_A - \omega_B)t} + \hat{a}\hat{b}^\dagger e^{-i(\omega_A - \omega_B)t}), \tag{8}$$

$$J_2 \to [J_{2,\rm dc} + J_{\rm ac}(e^{i\omega_m t} + e^{-i\omega_m t})] \times (\hat{a}^\dagger \hat{b}^\dagger e^{i(\omega_A + \omega_B)t} + \hat{a}\hat{b} e^{-i(\omega_A + \omega_B)t}), \tag{9}$$

where $J_{1,\rm dc} J_{2,\rm dc}$ are as in Eq. (4), and the strength of the modulated interaction may be approximated as

$$J_{\rm ac} \approx \frac{\pi \Phi_{\rm ac}}{4\sqrt{2}\Phi_0} \sin\left(\pi \frac{\Phi_{\rm dc}}{\Phi_0}\right) E_{J\max}^C \left(\frac{E_C^A E_C^B}{\widetilde{E}_J^A \widetilde{E}_J^B}\right)^{1/4}. \tag{10}$$

After applying the RWA, we may choose to activate either interaction with strength $J_{\rm ac}$ depending on the frequency of modulation, while other terms not commensurate with the modulation become fast-rotating and play a negligible role in the system dynamics. The full form of Eq. (10) and the contributions from higher-order interactions are shown in the Supplemental Material [44].

In order to measure the strength of the couplings under time-periodic pumping, we modulated the dc current supplied to the tunable coupler at a frequency $\omega_m$. The static component of the system under modulation can be written as

$$\hat{H}_{\rm dc} = \omega_A \hat{a}^\dagger \hat{a} + \frac{\alpha_A}{2} \hat{a}^\dagger \hat{a}^\dagger \hat{a}\hat{a} + \omega_B \hat{b}^\dagger \hat{b} + \frac{\alpha_B}{2} \hat{b}^\dagger \hat{b}^\dagger \hat{b}\hat{b} + V \hat{a}^\dagger \hat{a} \hat{b}^\dagger \hat{b}, \tag{11}$$

with additional terms present depending on the frequency at which the coupler flux is modulated. When modulating at the red sideband (RSB), we have

$$\hat{H}_{\rm RSB} = \hat{H}_{\rm dc} + \hat{H}_\Delta, \tag{12}$$

$$\hat{H}_\Delta = J_{\rm ac}(\hat{a}^\dagger \hat{b} + \hat{a}\hat{b}^\dagger), \tag{13}$$

and when modulating at the blue sideband (BSB), we similarly obtain

$$\hat{H}_{\rm BSB} = \hat{H}_{\rm dc} + \hat{H}_\Sigma, \tag{14}$$

$$\hat{H}_\Sigma = J_{\rm ac}(\hat{a}^\dagger \hat{b}^\dagger + \hat{a}\hat{b}), \tag{15}$$

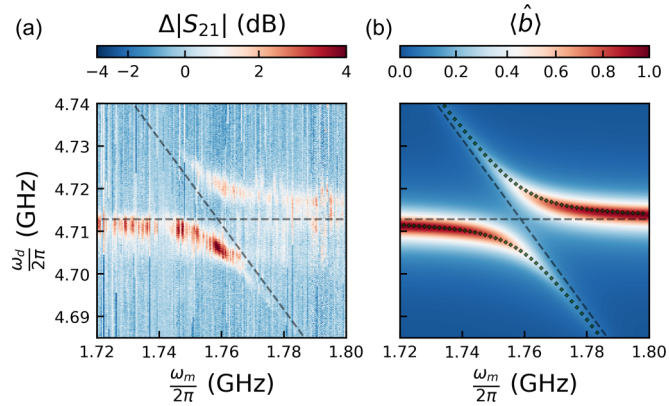


FIG. 2. Single-photon hopping interaction induced by red sideband flux modulation of the coupler. (a) Change in transmission while driving transmon $B$ and sweeping the modulation frequency of the dc signal incident on the tunable coupler through the red sideband of the two oscillators. The black dashed lines are guides for the eye. The horizontal dashed line is the first transition frequency of transmon $B$, and the diagonal dashed line is $(\omega_A - \omega_m)/2\pi$. (b) Eigenfrequencies obtained from fitting to the level repulsion model (markers) and the normalized expectation value of $\hat{b}$ obtained from a numerical quantum master equation simulation of the system.

with additional contributions to the total interaction strengths from correlated hopping and squeezing terms as discussed in the Supplemental Material [44].

## III. RESULTS

In Fig. 2, we set $\omega_A/2\pi = 6.472$ GHz, $\omega_B/2\pi = 4.713$ GHz, and $\Phi_{\rm dc} = 0.349\Phi_0$, and performed two-tone spectroscopy on transmon $B$ while sweeping $\omega_m/2\pi$ through $(\omega_A - \omega_B)/2\pi$. As the modulation frequency approached the red sideband of the oscillators, we observed an avoided crossing from which we extracted a single-photon hopping interaction strength of $J_{\rm ac}/2\pi = 7.462$ MHz and a cross-Kerr strength of $V/2\pi = -6.543$ MHz from a fit of the data. Fit parameters were found given our observed oscillator frequencies and interaction strengths from an analytical level repulsion model and by comparison to numerical quantum master equation simulations of the system. The magnitude of the observed splitting reflects the strength of the exchange interaction between the two oscillators at the resonance condition met under parametric modulation.

Similarly, in Fig. 3 we set $\omega_A/2\pi = 6.704$ GHz, $\omega_B/2\pi = 5.573$ GHz, and $\Phi_{\rm dc} = 0.215\Phi_0$, and performed two-tone spectroscopy on transmon $A$ while sweeping $\omega_m/2\pi$ through the cross-Kerr shifted sum frequency $(\omega_A + \omega_B + V)/2\pi$. As the pump frequency crossed the blue sideband, we observed features associated with the phenomenon of level attraction occurring between the two oscillators. Again, from an analytical model and numerical simulations, we extracted a two-mode squeezing strength of $J_{\rm ac}/2\pi = 1.131$ MHz and a cross-Kerr strength of $V/2\pi = -9.158$ MHz with an additional cross-Kerr shifted transition visible below the frequency of the primary oscillator response. The cross-Kerr coupling yields both a small peak in transmission below the primary transition feature due to thermal population of the oscillator

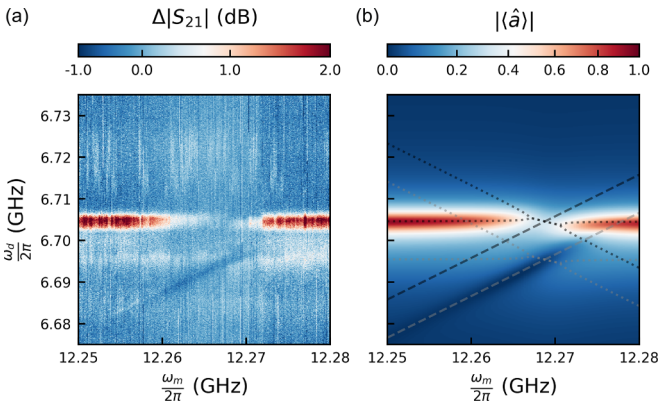


FIG. 3. Two-mode squeezing interaction induced by blue sideband flux modulation of the coupler. (a) Change in transmission while driving transmon $A$ and sweeping the modulation frequency of the dc bias incident on the tunable coupler through the blue sideband of the two oscillators. (b) The dashed lines are $(\omega_m - \omega_B)/2\pi$ and the same shifted vertically by $V/2\pi$. The dotted lines are the eigenfrequencies of the system determined from fits of the data to the analytical level attraction model. The underlying spectrum is the normalized expectation value of $\hat{a}$ obtained from a numerical simulation of a quantum master equation for the system.

mode, as well as the shifted level attraction feature visible as a decrease in transmission.

In the level attraction region where frequency degeneracy of the eigenmodes is theoretically predicted, we observed the primary resonance feature disappear. In this same region, we observed the emergence of a dip in the transmission spectrum related to a loss of excited-state population in transmon $A$. This absorption feature is shifted from the primary resonance by $V/2\pi$. It is associated with the microwave drive bringing the oscillator to its ground state from the excited state populated by the parametric modulation.

When modulating the flux through the coupler, the strength of the single-photon hopping and two-mode squeezing interactions is to first order linearly dependent on the amplitude of the modulation signal and thus can be tuned to lower or higher interaction strengths relative to the cross-Kerr for a wide range of static biases. The dependence of the interaction strengths on bias point and modulation amplitude is shown in Fig. 4(a), where the green region indicates the range of theoretically achievable cross-Kerr values depending on the flux bias points of the transmons and coupler. In contrast, the gray region shows the viable values of $J_{ac}/2\pi$ for a range of modulation strengths.

While we demonstrated the ability to enter into this cross-Kerr dominant coupling regime, we also observed two-mode squeezing interactions, which are typically far off-resonant and fast-rotating in the frame of the oscillators. This entangling interaction generates coupled signal and idler modes and has been used to perform two-qubit gate (bswap) operations in the truncated qubit subspace [14,45–47]. Activating this term enables the tuning of XX-YY interactions between the oscillators, broadening the array of systems such devices can effectively simulate. The modulated strength is tunable over a wide range, enabling the possibility for simulation of arbitrary XYZ spin-model Hamiltonians when coupled with the controllability demonstrated by the XX+YY and ZZ interactions [30].

Prospects for bichromatic flux pumps are also promising, where phase differences between simultaneously applied red

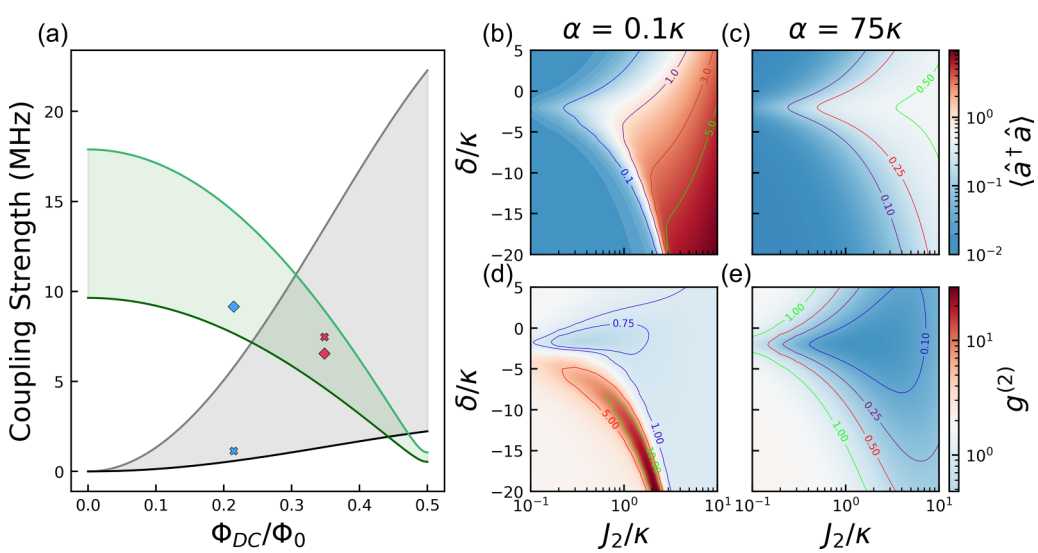


FIG. 4. Interaction strengths and distinct response parameter regimes. (a) The calculated interaction strengths as the dc flux bias point of the coupler is changed. The gradient of curves in green shows the possible values of the cross-Kerr interaction for the range of $\Phi_{A,B} \in [0.0, 0.5\Phi_0]$ at each value of $\Phi_{dc}$. The gradient of curves in gray shows the values of single-photon hopping or two-mode squeezing interactions for a range of modulation strengths between $\Phi_{ac} = \Phi_{dc}/100$ and $\Phi_{ac} = \Phi_{dc}/10$. The diamond ($V/2\pi$) and cross ($J_{ac}/2\pi$) markers indicate the extracted interaction strengths from Figs. 2 (red) and 3 (blue). (b), (c) The photon number expectation value for one mode of a system of two coupled Kerr-nonlinear oscillators subject to a drive-induced two-mode squeezing interaction where the strength of the interaction $J_2$, detuning of the drive from the sum frequency resonance condition $\delta$, and nonlinearity $\alpha$ are varied relative to the loss rates of the oscillators $\kappa$. (d), (e) The second-order correlation function of one of the oscillators as in panels (b) and (c).

and blue sideband pumps would allow for pure XX or YY interactions [30]. Such driven coupler schemes have been previously investigated in the context of Floquet engineering, in which tunable and selectively activatable interactions are integral to the proposed analog quantum simulation of Kitaev honeycomb models [30]. The nonstoquastic terms that a parametrically modulated tunable coupler can contribute to the system are also of great interest with respect to the study of possible quantum advantage over classical approaches in annealing protocols [24,48,49].

These parametric interactions additionally provide insight into the dual phenomena of level repulsion and attraction. The red and blue sideband results illustrate the ability to transition between coherent (real) coupling and dissipative (imaginary) coupling simply with an applied modulation pump. Such couplings have long been the focus of study in magnonic, Bose-Einstein condensate, and optomechanical systems, typically operating in regimes where the nonlinearities of the oscillators are small [40–42,50–56].

In the case of level attraction, a system of coupled linear oscillators exhibits a region of parametric instability with two exceptional points indicating the transition of the system to one with complex eigenfrequencies with opposite-sign imaginary components. In this situation, one eigenmode grows exponentially and becomes unstable while the other decays exponentially. Such a situation arises only when the dissipation rates of the two oscillator modes are commensurate and the coupling exceeds the oscillator decay rates [40]. For our two oscillators, the linewidths are each on the order of a few megahertz for the flux points investigated, and the coupling strength can be tuned to less than or greater than the dissipation rates for typical transmon coherence times given the choice of modulation amplitude.

The same interaction was also previously observed between two coupled weakly nonlinear modes of a SQUID-terminated coplanar waveguide resonator subject to flux modulation [45]. Nondegenerate parametric oscillations were observed when the system was driven beyond the parametric instability threshold for a range of sufficient detunings and modulation strengths. In these systems, the self-Kerr and cross-Kerr couplings of the modes were often smaller than the decay rates, with large photon number states generable when driven above threshold [45,46,57,58]. Upon the application of an additional drive, such parametric oscillators can also become injection-locked to the drive [59].

The main distinctions between the behavior outlined above and what we observe in Fig. 3 are that the oscillators measured are strongly nonlinear and that we do not observe a region of parametric instability due to the low strength of the two-mode squeezing interaction relative to the self-Kerr-nonlinearities of the oscillators. Further, our oscillators are additionally cross-Kerr coupled, which yields a frequency shift of the spectroscopic features. In order to investigate these distinctions and better understand the contributions of the self-Kerr and cross-Kerr terms to the phenomenon of level attraction between strongly nonlinear oscillators, we numerically simulated the system for a variety of parameters.

In Figs. 4(b)–4(e), we show for one mode the photon number expectation values $\langle a^\dagger a\rangle$ and second-order correlation function $g^{(2)}$ in a system of two Kerr-nonlinear oscillators as in Eq. (14), where the correlated squeezing terms are set to zero, determined from quantum master equation simulations [60]. We set $V = -2\kappa$ and vary the strength of the two-mode squeezing term $J_2$ and detuning of the modulation frequency from the sum frequency resonance condition $\delta$ for the case of weakly nonlinear oscillators $\alpha = 0.1\kappa$ and strongly nonlinear oscillators $\alpha = 75\kappa$. For the weakly nonlinear system, as the strength of the two-mode squeezing interaction increases, the parametric response region, which provides an increased photon number, shifts to large, negative detunings. Additionally, a sudden peak in $g^{(2)}$ bounds the parametric response region from below, which is a known marker of a phase transition in KNOs [61].

In contrast, for strongly nonlinear oscillators, such as transmon qubits, for $J_2 < \alpha$ and in a region centered about the cross-Kerr shifted sum frequency resonance condition, the photon number expectation and second-order correlation function remain below one. In this case, the two-mode squeezing interaction acts effectively on the qubit subspace alone, generating an XX-YY interaction. The large self-Kerr-nonlinearities of the oscillators prevent the system from reaching a parametric instability as in the case of the linear and weakly nonlinear two-mode squeezed systems, instead generating a low photon number entangled state.

## IV. SUMMARY—OUTLOOK

In summary, we have demonstrated the operation of a transmon-based circuit containing a flux-tunable coupler enabling access into different coupling regimes, including cross-Kerr couplings ($V$), between two nonlinear oscillators. By parametrically modulating the inductance of the coupler SQUID loop with an applied time-dependent magnetic field, we can selectively activate either a single-photon hopping coupling ($J_1$) or two-mode squeezing coupling ($J_2$) between two transmon qubits. The coupling strengths can be tuned by choosing different dc flux bias points and modulation amplitude. In combination with previously reported measurements of strong resonant single-photon hopping interactions on this device [10], this scheme gives access to parameter regimes where $J_{1,2} > V$, $J_{1,2} \approx V$, and $J_{1,2} < V$.

This tunability allows for the simulation of various systems, including Ising ZZ, Bose-Hubbard, and Heisenberg XXZ models [4,5,25,30]. The ability to tune into and out of these regimes is of particular interest for analog quantum simulations, where such superconducting devices can be made to emulate a variety of physical systems with solely *in situ* control and a broad range of coupling strengths achievable. A minimal configuration for useful analog quantum simulations in a two-dimensional grid would require at least four interconnected KNOs. This could realize a honeycomb cell prototype emulating the Kitaev model [30] or the frustrated Ising model [25]. Furthermore, a closed-loop plaquette of interconnected KNOs would give rise to ring-exchange interactions for a minimal quantum simulation of lattice gauge theories [27]. While useful quantum simulations can be performed in a system of $N = 4$, surpassing classical computers in simulating these problems would require scaling to $N > 50$, which is feasible with state-of-the-art devices [3]. In addition, as reported in Ref. [10], this tunable coupler does not limit the transmon

coherence, which, together with recent modular tunable coupling realizations [62], holds great promise for scaling up to larger lattices.

Moreover, our circuit model predicts that further measurements using modulated couplers operating in different conditions may be used to activate more regimes, such as photon-pair tunneling, correlated photon hopping, and photon-pressure interactions. Using asymmetric nonlinear elements would also enable the simulation of more exotic interactions and simultaneously enable tuning of several device parameters, such as self-Kerr terms, which can be tuned from negative to positive values [39,63]. The broad selectivity of system parameters in tunably coupled nonlinear oscillators is of particular interest due to the ability to investigate instability regimes, applications to parametric amplification, driven-dissipative interactions, as well as exploring non-Hermitian Hamiltonians [5,64,65]. Exquisite control over these interactions would enable direct investigation of coherent and dissipative couplings between nonlinear oscillators and bring predicted applications in topological energy transfer, quantum sensing, and nonreciprocal photon transmission closer to experimental realization [53,54,56,66,67].

Finally, under tunable blue sideband modulation, we have observed level attraction between the two nonlinear oscillators. Interestingly, the behavior of the system differs from previously established theoretical descriptions and experimental observations of linear systems exhibiting level attraction [40–42]. Using an extension of existing methods and numerical simulations, we were able to determine that the cross-Kerr coupling yields an additional shifted spectroscopic feature of level attraction and that signatures of level attraction can be observed in the absence of parametric instability in the case of strongly Kerr-nonlinear oscillators. The dual phenomena of level repulsion and level attraction have been previously investigated in a broad array of platforms ranging from Bose-Einstein condensates to magnonic and optomechanical systems operating in various parameter regimes characterized by the resonance frequencies, coupling strengths, and decay rates of the constituent oscillators [40–42,50–55,68–71]. Furthermore, dissipative couplings and two-mode squeezing interactions giving rise to level attraction are particularly useful for enabling quantum-limited nondegenerate parametric amplification as well as performing two-qubit gate operations [14,45,68].

## ACKNOWLEDGMENTS

J.D.K., M.K., and G.A.S. acknowledge financial support by the EU program H2020-FETOPEN Project No. 828826 Quromorphic. M.K. acknowledges financial support from the Netherlands Organisation for Scientific Research (NWO/OCW). C.A.P. acknowledges the support of the Novo Nordisk Foundation, Grant No. NNF22SA0081175, NNF Quantum Computing Programme.

J.D.K., G.B., and M.K. carried out the theoretical analysis. M.K. designed and fabricated the device in the group of Leo DiCarlo. J.D.K., F.F.S, and M.K. conducted the measurements. J.D.K and G.B. performed the simulations. M.K. and G.A.S. conceived the experiment. C.A.P., M.K., and G.A.S. supervised the project. J.D.K. and M.K. wrote the manuscript with input from all authors.

## DATA AVAILABILITY

The data that support the findings of this article are openly available [72].

[1] J. Koch, T. M. Yu, J. Gambetta, A. A. Houck, D. I. Schuster, J. Majer, A. Blais, M. H. Devoret, S. M. Girvin, and R. J. Schoelkopf, Charge-insensitive qubit design derived from the Cooper pair box, Phys. Rev. A **76**, 042319 (2007).

[2] P. J. J. O'Malley, R. Babbush, I. D. Kivlichan, J. Romero, J. R. McClean, R. Barends, J. Kelly, P. Roushan, A. Tranter, N. Ding, *et al.*, Scalable quantum simulation of molecular energies, Phys. Rev. X **6**, 031007 (2016).

[3] F. Arute, K. Arya, R. Babbush, D. Bacon, J. C. Bardin, R. Barends, R. Biswas, S. Boixo, F. G. S. L. Brandao, D. A. Buell, *et al.*, Quantum supremacy using a programmable superconducting processor, Nature (London) **574**, 505 (2019).

[4] I. M. Georgescu, S. Ashhab, and F. Nori, Quantum simulation, Rev. Mod. Phys. **86**, 153 (2014).

[5] M. J. Hartmann, Quantum simulation with interacting photons, J. Opt. **18**, 104005 (2016).

[6] S. Mostame, J. Huh, C. Kreisbeck, A. J. Kerman, T. Fujita, A. Eisfeld, and A. Aspuru-Guzik, Emulation of complex open quantum systems using superconducting qubits, Quantum Info. Proc. **16**, 44 (2017).

[7] S. A. Wilkinson and M. J. Hartmann, Superconducting quantum many-body circuits for quantum simulation and computing, Appl. Phys. Lett. **116**, 230501 (2020).

[8] A. O. Niskanen, Y. Nakamura, and J.-S. Tsai, Tunable coupling scheme for flux qubits at the optimal point, Phys. Rev. B **73**, 094506 (2006).

[9] Y. Chen, C. Neill, P. Roushan, N. Leung, M. Fang, R. Barends, J. Kelly, B. Campbell, Z. Chen, B. Chiaro, *et al.*, Qubit architecture with high coherence and fast tunable coupling, Phys. Rev. Lett. **113**, 220502 (2014).

[10] M. Kounalakis, C. Dickel, A. Bruno, N. K. Langford, and G. A. Steele, Tuneable hopping and nonlinear cross-Kerr interactions in a high-coherence superconducting circuit, npj Quantum Inf. **4**, 38 (2018).

[11] F. Yan, P. Krantz, Y. Sung, M. Kjaergaard, D. L. Campbell, T. P. Orlando, S. Gustavsson, and W. D. Oliver, Tunable coupling scheme for implementing high-fidelity two-qubit gates, Phys. Rev. Appl. **10**, 054062 (2018).

[12] M. R. Geller, E. Donate, Y. Chen, M. T. Fang, N. Leung, C. Neill, P. Roushan, and J. M. Martinis, Tunable coupler for superconducting Xmon qubits: Perturbative nonlinear model, Phys. Rev. A **92**, 012320 (2015).

[13] D. C. McKay, S. Filipp, A. Mezzacapo, E. Magesan, J. M. Chow, and J. M. Gambetta, Universal gate for fixed-frequency qubits via a tunable bus, Phys. Rev. Appl. **6**, 064007 (2016).

[14] M. Roth, M. Ganzhorn, N. Moll, S. Filipp, G. Salis, and S. Schmidt, Analysis of a parametrically driven exchange-type gate and a two-photon excitation gate between superconducting qubits, Phys. Rev. A **96**, 062323 (2017).

[15] M. C. Collodo, J. Herrmann, N. Lacroix, C. K. Andersen, A. Remm, S. Lazar, J.-C. Besse, T. Walter, A. Wallraff, and C. Eichler, Implementation of conditional phase gates based on tunable *ZZ* interactions, Phys. Rev. Lett. **125**, 240502 (2020).

[16] T. Miyanaga, A. Tomonaga, H. Ito, H. Mukai, and J. S. Tsai, Ultrastrong tunable coupler between superconducting *LC* resonators, Phys. Rev. Appl. **16**, 064041 (2021).

[17] J. Stehlik, D. M. Zajac, D. L. Underwood, T. Phung, J. Blair, S. Carnevale, D. Klaus, G. A. Keefe, A. Carniol, M. Kumph, M. Steffen, and O. E. Dial, Tunable coupling architecture for fixed-frequency transmon superconducting qubits, Phys. Rev. Lett. **127**, 080505 (2021).

[18] Y. Sung, L. Ding, J. Braumüller, A. Vepsäläinen, B. Kannan, M. Kjaergaard, A. Greene, G. O. Samach, C. McNally, D. Kim, A. Melville, B. M. Niedzielski, M. E. Schwartz, J. L. Yoder, T. P. Orlando, S. Gustavsson, and W. D. Oliver, Realization of high-fidelity CZ and *ZZ*-free iSWAP gates with a tunable coupler, Phys. Rev. X **11**, 021058 (2021).

[19] L. Heunisch, C. Eichler, and M. J. Hartmann, Tunable coupler to fully decouple and maximally localize superconducting qubits, Phys. Rev. Appl. **20**, 064037 (2023).

[20] N. Janzen, X. Dai, S. Ren, J. Shi, and A. Lupascu, Tunable coupler for mediating interactions between a two-level system and a waveguide from a decoupled state to the ultrastrong coupling regime, Phys. Rev. Res. **5**, 033155 (2023).

[21] N. J. Glaser, F. Roy, and S. Filipp, Controlled-controlled-phase gates for superconducting qubits mediated by a shared tunable coupler, Phys. Rev. Appl. **19**, 044001 (2023).

[22] R. Li, K. Kubo, Y. Ho, Z. Yan, Y. Nakamura, and H. Goto, Realization of high-fidelity CZ gate based on a double-transmon coupler, Phys. Rev. X **14**, 041050 (2024).

[23] G. Corrielli, A. Crespi, G. Della Valle, S. Longhi, and R. Osellame, Fractional Bloch oscillations in photonic lattices, Nat. Commun. **4**, 1555 (2013).

[24] J. Jin, D. Rossini, R. Fazio, M. Leib, and M. J. Hartmann, Photon solid phases in driven arrays of nonlinearly coupled cavities, Phys. Rev. Lett. **110**, 163605 (2013).

[25] S. Jin, A. Sen, W. Guo, and A. W. Sandvik, Phase transitions in the frustrated Ising model on the square lattice, Phys. Rev. B **87**, 144406 (2013).

[26] D. Marcos, P. Rabl, E. Rico, and P. Zoller, Superconducting circuits for quantum simulation of dynamical gauge fields, Phys. Rev. Lett. **111**, 110504 (2013).

[27] D. Marcos, P. Widmer, E. Rico, M. Hafezi, P. Rabl, U.-J. Wiese, and P. Zoller, Two-dimensional lattice gauge theories with superconducting quantum circuits, Ann. Phys. **351**, 634 (2014).

[28] A. S. Dehkharghani, E. Rico, N. T. Zinner, and A. Negretti, Quantum simulation of Abelian lattice gauge theories via state-dependent hopping, Phys. Rev. A **96**, 043611 (2017).

[29] M. Sameti, A. Potočnik, D. E. Browne, A. Wallraff, and M. J. Hartmann, Superconducting quantum simulator for topological order and the toric code, Phys. Rev. A **95**, 042330 (2017).

[30] M. Sameti and M. J. Hartmann, Floquet engineering in superconducting circuits: From arbitrary spin-spin interactions to the Kitaev honeycomb model, Phys. Rev. A **99**, 012333 (2019).

[31] I. T. Rosen, S. Muschinske, C. N. Barrett, A. Chatterjee, M. Hays, M. A. DeMarco, A. H. Karamlou, D. A. Rower, R. Das, D. K. Kim, B. M. Niedzielski, M. Schuldt, K. Serniak, M. E. Schwartz, J. L. Yoder, J. A. Grover, and W. D. Oliver, A synthetic magnetic vector potential in a 2D superconducting qubit array, Nat. Phys. **20**, 1881 (2024).

[32] N. Didier, J. Bourassa, and A. Blais, Fast quantum nondemolition readout by parametric modulation of longitudinal qubit-oscillator interaction, Phys. Rev. Lett. **115**, 203601 (2015).

[33] I. C. Rodrigues, D. Bothner, and G. A. Steele, Cooling photon-pressure circuits into the quantum regime, Sci. Adv. **7**, eabg6653 (2021).

[34] C. A. Potts, R. C. Dekker, S. Deve, E. W. Strijbis, and G. A. Steele, Strong intrinsic longitudinal coupling in circuit quantum electrodynamics, Phys. Rev. Lett. **134**, 153603 (2025).

[35] M. Kounalakis, G. E. W. Bauer, and Y. M. Blanter, Analog quantum control of magnonic cat states on a chip by a superconducting qubit, Phys. Rev. Lett. **129**, 037205 (2022).

[36] M. Kounalakis, S. Viola Kusminskiy, and Y. M. Blanter, Engineering entangled coherent states of magnons and phonons via a transmon qubit, Phys. Rev. B **108**, 224416 (2023).

[37] Y. Salathé, M. Mondal, M. Oppliger, J. Heinsoo, P. Kurpiers, A. Potočnik, A. Mezzacapo, U. Las Heras, L. Lamata, E. Solano, S. Filipp, and A. Wallraff, Digital quantum simulation of spin models with circuit quantum electrodynamics, Phys. Rev. X **5**, 021027 (2015).

[38] S. Puri, C. K. Andersen, A. L. Grimsmo, and A. Blais, Quantum annealing with all-to-all connected nonlinear oscillators, Nat. Commun. **8**, 15785 (2017).

[39] N. E. Frattini, U. Vool, S. Shankar, A. Narla, K. M. Sliwa, and M. H. Devoret, 3-wave mixing Josephson dipole element, Appl. Phys. Lett. **110**, 222603 (2017).

[40] N. R. Bernier, L. D. Tóth, A. K. Feofa11, and T. J. Kippenberg, Level attraction in a microwave optomechanical circuit, Phys. Rev. A **98**, 023841 (2018).

[41] Y.-P. Wang, J. W. Rao, Y. Yang, P.-C. Xu, Y. S. Gui, B. M. Yao, J. Q. You, and C.-M. Hu, Nonreciprocity and unidirectional invisibility in cavity magnonics, Phys. Rev. Lett. **123**, 127202 (2019).

[42] W. Yu, J. Wang, H. Y. Yuan, and J. Xiao, Prediction of attractive level crossing via a dissipative mode, Phys. Rev. Lett. **123**, 227201 (2019).

[43] M. D. Hutchings, J. B. Hertzberg, Y. Liu, N. T. Bronn, G. A. Keefe, M. Brink, J. M. Chow, and B. L. T. Plourde, Tunable superconducting qubits with flux-independent coherence, Phys. Rev. Appl. **8**, 044003 (2017).

[44] See Supplemental Material at http://link.aps.org/supplemental/10.1103/3pf2-8n9b for a full description of the measurement setup, as well as the theoretical analysis, including the full circuit quantization and extraction of the relevant coupling terms, which also includes Refs. [73,74].

[45] A. Bengtsson, P. Krantz, M. Simoen, I.-M. Svensson, B. Schneider, V. Shumeiko, P. Delsing, and J. Bylander, Nondegenerate parametric oscillations in a tunable superconducting resonator, Phys. Rev. B **97**, 144502 (2018).

[46] W. Wustmann and V. Shumeiko, Parametric effects in circuit quantum electrodynamics, Low Temp. Phys. **45**, 848 (2019).

[47] S. Poletto, J. M. Gambetta, S. T. Merkel, J. A. Smolin, J. M. Chow, A. D. Córcoles, G. A. Keefe, M. B. Rothwell, J. R. Rozen, D. W. Abraham, C. Rigetti, and M. Steffen, Entanglement of two superconducting qubits in a waveguide cavity via monochromatic two-photon excitation, Phys. Rev. Lett. **109**, 240505 (2012).

[48] L. Hormozi, E. W. Brown, G. Carleo, and M. Troyer, Nonstoquastic Hamiltonians and quantum annealing of an Ising spin glass, Phys. Rev. B **95**, 184416 (2017).

[49] A. Ciani and B. M. Terhal, Stoquasticity in circuit QED, Phys. Rev. A **103**, 042401 (2021).

[50] N. R. Bernier, E. G. Dalla Torre, and E. Demler, Unstable avoided crossing in coupled spinor condensates, Phys. Rev. Lett. **113**, 065303 (2014).

[51] H. Xu, D. Mason, L. Jiang, and J. G. E. Harris, Topological energy transfer in an optomechanical system with exceptional points, Nature (London) **537**, 80 (2016).

[52] D. Zhang, X.-Q. Luo, Y.-P. Wang, T.-F. Li, and J. Q. You, Observation of the exceptional point in cavity magnon-polaritons, Nat. Commun. **8**, 1368 (2017).

[53] M. Harder, Y. Yang, B. M. Yao, C. H. Yu, J. W. Rao, Y. S. Gui, R. L. Stamps, and C.-M. Hu, Level attraction due to dissipative magnon-photon coupling, Phys. Rev. Lett. **121**, 137203 (2018).

[54] B. Bhoi, B. Kim, S.-H. Jang, J. Kim, J. Yang, Y.-J. Cho, and S.-K. Kim, Abnormal anticrossing effect in photon-magnon coupling, Phys. Rev. B **99**, 134426 (2019).

[55] Y. Yang, J. W. Rao, Y. S. Gui, B. M. Yao, W. Lu, and C.-M. Hu, Control of the magnon-photon level attraction in a planar cavity, Phys. Rev. Appl. **11**, 054023 (2019).

[56] B. Yao, T. Yu, X. Zhang, W. Lu, Y. Gui, C.-M. Hu, and Y. M. Blanter, The microscopic origin of magnon-photon level attraction by traveling waves: Theory and experiment, Phys. Rev. B **100**, 214426 (2019).

[57] W. Wustmann and V. Shumeiko, Parametric resonance in tunable superconducting cavities, Phys. Rev. B **87**, 184501 (2013).

[58] W. Wustmann and V. Shumeiko, Nondegenerate parametric resonance in a tunable superconducting cavity, Phys. Rev. Appl. **8**, 024018 (2017).

[59] D. Marković, J. D. Pillet, E. Flurin, N. Roch, and B. Huard, Injection locking and parametric locking in a superconducting circuit, Phys. Rev. Appl. **12**, 024034 (2019).

[60] J. Johansson, P. Nation, and F. Nori, QuTiP 2: A Python framework for the dynamics of open quantum systems, Comput. Phys. Commun. **184**, 1234 (2013).

[61] N. Bartolo, F. Minganti, W. Casteels, and C. Ciuti, Exact steady state of a Kerr resonator with one- and two-photon driving and dissipation: Controllable Wigner-function multimodality and dissipative phase transitions, Phys. Rev. A **94**, 033841 (2016).

[62] M. Field, A. Q. Chen, B. Scharmann, E. A. Sete, F. Oruc, K. Vu, V. Kosenko, J. Y. Mutus, S. Poletto, and A. Bestwick, Modular superconducting-qubit architecture with a multichip tunable coupler, Phys. Rev. Appl. **21**, 054063 (2024).

[63] Y. Lu, M. Kudra, T. Hillmann, J. Yang, H.-X. Li, F. Quijandría, and P. Delsing, Resolving Fock states near the Kerr-free point of a superconducting resonator, npj Quantum Inf. **9**, 114 (2023).

[64] A. Metelmann and A. A. Clerk, Quantum-limited amplification via reservoir engineering, Phys. Rev. Lett. **112**, 133904 (2014).

[65] H. M. Hurst and B. Flebus, Non-Hermitian physics in magnetic systems, J. Appl. Phys. **132**, 220902 (2022).

[66] J. Kohler, J. A. Gerber, E. Dowd, and D. M. Stamper-Kurn, Negative-mass instability of the spin and motion of an atomic gas driven by optical cavity backaction, Phys. Rev. Lett. **120**, 013601 (2018).

[67] N. R. Bernier, L. D. Tóth, A. K. Feofanov, and T. J. Kippenberg, Nonreciprocity in microwave optomechanical circuits, IEEE Antennas Wirel. Propag. Lett. **17**, 1983 (2018).

[68] C. Eichler, Y. Salathe, J. Mlynek, S. Schmidt, and A. Wallraff, Quantum-limited amplification and entanglement in coupled nonlinear resonators, Phys. Rev. Lett. **113**, 110502 (2014).

[69] V. L. Grigoryan, K. Shen, and K. Xia, Synchronized spin-photon coupling in a microwave cavity, Phys. Rev. B **98**, 024406 (2018).

[70] M.-A. Miri and A. Alù, Exceptional points in optics and photonics, Science **363**, eaar7709 (2019).

[71] Y.-P. Wang and C.-M. Hu, Dissipative couplings in cavity magnonics, J. Appl. Phys. **127**, 130901 (2020).

[72] J. Koenig, Data and scripts underlying the PhD thesis: Parametrically activated interactions in circuit quantum electrodynamical systems, 4TU.ResearchData (2024), https://doi.org/10.4121/0d0ef8aa-43d9-46ab-8afd-e02b76f2469a.

[73] N. Didier, E. A. Sete, M. P. da Silva, and C. Rigetti, Analytical modeling of parametrically modulated transmon qubits, Phys. Rev. A **97**, 022330 (2018).

[74] S. A. Caldwell, N. Didier, C. A. Ryan, E. A. Sete, A. Hudson, P. Karalekas, R. Manenti, M. P. da Silva, R. Sinclair, E. Acala, *et al.*, Parametrically activated entangling gates using transmon qubits, Phys. Rev. Appl. **10**, 034050 (2018).